JOURNAL OF MORPHOLOGY 220:185–205 (1994)

Comparative Morphology of the Myomeres and Axial Skeleton in Four Genera of Centrarchid Fishes

BRUCE C. JAYNE AND GEORGE V. LAUDER
Department of Biological Sciences, University of Cincinnati, Cincinnati, Ohio 45221-0006 (B.C.J.); Department of Ecology and Evolutionary Biology, University of California, Irvine, California 92717 (G.V.L.)

ABSTRACT We used X-rays and dissection of myotomes to quantify the axial morphology of four species of centrarchid fishes (*Micropterus salmoides, Ambloplites rupestris, Pomoxis nigromaculatus,* and *Lepomis macrochirus*). Proceeding from dorsal to ventral, we designated the two epaxial and two hypaxial portions of the myomeres AB, BC, CD, and DE, respectively. For each of 11 myomeres, spaced at 10% increments along the length of the fish, a total of 14 variables described the length and orientation of each portion, the dorsal-ventral symmetry, and the overall height and longitudinal span of the entire myomere. Nine variables described the lengths, orientation, and symmetry of the vertebral centra, neural and hemal spines, and ribs. Analysis of variance revealed that, with one exception, all 23 morphological variables varied significantly both among species and among longitudinal locations within a species. However, the extent of longitudinal and interspecific variance differed considerably among different variables. Maximal myomeric height ranged from about 45% of the standard length (SL) in *Lepomis* to 27% SL in *Micropterus*. Longitudinal and interspecific increases in overall height of the trunk myomeres resulted primarily from greater lengths of CD. Compared to other portions of the myomere, the length of BC was most conservative both longitudinally and interspecifically. Dorsal-ventral symmetry of the myomeres and axial skeleton was greater in the caudal region than in the trunk in all species, and the myomeric morphology diverged least among species in the posterior caudal region. The overall longitudinal span of superficial myomeric landmarks varied from 6% to 18% SL, and, including the deep portions of the myomeres, the longitudinal span varied from about 7 to 10 vertebrae. Within each of the species, myomeric and skeletal variables were often not significantly correlated, but for the pooled data of all species there were usually highly significant correlations between myomeric and skeletal morphology. For example, strong correlations existed between BC and the underlying neural spines, and between CD and the underlying ribs and hemal spines. In contrast, the longitudinal spans of entire myomeres and underlying axial skeletal segments were only weakly associated.

Many of the most influential studies in fish locomotion over the last 30 years have involved a fruitful combination of hydrodynamic modeling, kinematics, and analyses of external body shape (Webb, '75; '78a; Weihs and Webb, '83). For example, Webb (e.g., '78b, '82) has clarified how hydrodynamic performance is related to the distribution of external body surface area in different species. In contrast, scant information presently relates interspecific variation in external shape to variation in the internal axial morphology. Furthermore, longitudinal variation in the axial musculature and skeleton within the body of individual fish generally has not been quantified despite the fact the such variation has significant consequences for understanding how locomotor forces are generated and transmitted. Some studies of longitudinal and interspecific variation in the axial morphology and function of fishes have examined the importance of myotomal fiber

trajectories (Alexander, '69), biomechanical properties such as stiffness (Blight, '77; Wainwright, '83; Long, '92), and muscle strain (Van Leeuwen et al., 1990; Altringham et al., '93; Rome et al., '93). Only recently (Westneat et al., '93) have studies begun to quantify both intraspecific longitudinal variation and interspecific variation in the axial structures that are relevant to understanding locomotor function. Especially lacking are quantitative studies of the overall shape of myotomes and their relationship to the axial skeleton.

The description of axial morphology is critical to understanding locomotor mechanics for at least three reasons. First, a single myotome may span many vertebrae and thus potentially induce bending at many segments simultaneously. Although Greene and Greene ('14) state that a single myotome in the salmon may span more than ten vertebrae, there are no comparable data for other taxa to indicate myotomal spans, nor are there any data to indicate how myotomal span changes down the length of the body. To relate patterns of electrical activity in myotomes to patterns of body deformation, it is essential to know how many vertebral segments might be affected by myotomal fiber contraction. Second, the fish myotome changes shape considerably along the body, and these changes in shape will affect the transmission of force to the axial skeleton. However, there are no published measurements of longitudinal shape changes in the myotomes of fishes. Third, the relationship between the axial skeleton (neural and hemal spines and vertebral centra) and myotomes may also change along the body, yet there is little information available on skeletal-myotomal relationships.

Previous structural research on fish myotomes has focused on considering fiber types and their innervation and spatial distribution (e.g., Waterman, '69; Bone, '78; Westerfield et al., '86), and on general descriptions of the position of one or a few myotomes within the body (Harder, '75; Lindsey '78). In addition, the phylogenetic distribution of the taxa illustrated has varied widely. Nursall ('56) illustrated myomeric shape for *Branchiostoma,* a lamprey, one shark, and one bony fish. Additional illustrations of myomeres in osteichthyians are available for *Tilapia* (Vidleler, '75), salmon (Greene and Greene, '14), and a sea trout (Wainwright, '83). Most recently, Westneat et al. ('93) described the lengths and orientations of various connective tissue structures associated with myotomes, and they described differences in the axial musculature that were associated with the specialized tails that are found in several species of scombrid fishes.

The general aim of this study was to quantify myomeric and skeletal morphology in a few fish taxa that vary significantly in body shape within a relatively small monophyletic clade. To this end, we chose the endemic North American sunfish family Centrarchidae. The centrarchid fishes are a well-defined monophyletic clade of perciform teleost fishes (Lauder and Liem, '83; Mabee, '93) that vary considerably in their external shape while having only slight variation in the number of vertebrae (Mabee, '93; Scott and Crossman, '73). For example, the bass (*Micropterus*) is fusiform in both the sagittal and frontal planes (Webb, '84), while the genus *Lepomis* is laterally flattened and contains species with deep bodies approximating one-third of body length: Both taxa possess about 30 vertebrae. An additional reason for choosing centrarchid fishes is our parallel and ongoing investigation of locomotion, involving both kinematic and electromyographic studies of steady and unsteady behaviors (Gibb et al., '94; Jayne and Lauder, '91, '93, '94). Thus, we plan to integrate the morphological data presented here with subsequent analyses of locomotor kinematics and myotomal muscle function.

The specific goals of this study were 1) to quantify longitudinal variation in axial morphology for the four centrarchid genera chosen for detailed analysis (*Micropterus, Ambloplites, Pomoxis,* and *Lepomis*), 2) to compare axial morphology among the taxa, and 3) to correlate differences in external shape (body depth) with the internal shapes of the myomeres and axial skeleton. We also consider whether all portions of the myomeres varied equally or if certain portions of the myomere are morphologically more plastic than other portions.

MATERIALS AND METHODS

We examined the axial morphology of five specimens for each of four species of centrarchid fishes (*Micropterus salmoides, Ambloplites rupestris, Pomoxis nigromaculatus,* and *Lepomis macrochirus*). Within each species, specimens were from the same population, but not all of the species were from the same collection sites. When possible, we selected specimens with similar standard lengths (SL),

which ranged from 110 to 167 mm for the entire sample of 20 individuals; the mean values of SL for each species ranged from 139 to 158 mm (Table 1). All specimens had been previously fixed in formalin and were stored in 70% ethanol at the time of the dissections, and we selected individuals with no conspicuous lateral or dorsal flexion of the vertebral column.

To expose the lateral surface of the myomeres, we removed the skin from the entire left side of each fish. We removed a parasagittal section from the right side of the fish so that the left portion of the specimen would sit flat when it was pinned onto a sheet of styrofoam approximately 2 cm thick. The four superficial portions of myomeres and myosepta of fish resemble a W-shape, for which the top is oriented anteriorly and the middle is on the horizontal septum. We cut number 0 Asta insect pins with steel heads to convenient lengths, and then inserted them at the five landmarks of each myoseptum that corresponded to the most anterior and posterior ends of each of the four portions of the myoseptum (Figs. 1, 2). To provide a distance scale, additional pins were placed 5 cm apart in the styrofoam block, and these pins protruded above the styrofoam approximately the same height as the average level of the pinheads at the myomere landmarks. We then obtained lateral view X-rays of the preparations with a veterinary unit using a source to object distance of ca. 50 cm and an exposure of 21 mAs and 42 kvp; we used an Optex detail screen and Konica medical X-ray film. For the images shown in Figures 1 and 2 we used Kodak Industrex film exposed in a Hewlett Packard Faxitron X-ray system.

To quantify the morphology of the myomeres and axial skeleton, the X-ray films were placed on a light table and a video image was obtained using a Javelin CCD video camera. A digital file of each video image was later displayed on a video monitor at more than twice life size when we digitized coordinates. Our custom software had a movable cursor in the video display which was used to record the coordinates of anatomical landmarks from the video image. In preliminary work, we used a square reference grid to verify that this combination of software and video display provided undistorted images and coordinates (ca. ±0.5 mm). All X-ray images were oriented so that the longitudinal axis of the specimen was parallel to the X-axis of the digitizing coordinate system. The longitudinal axis of the fish was defined as a straight line passing through the middle of centra of the most posterior complete caudal vertebrae and passing along the ventral margin of the parasphenoid bone of the braincase.

On the digitally reconstructed images, the five landmarks within each myoseptum were then connected with a series of four straight-line segments as shown in Figures 3 and 4. We labeled these landmarks A through E, proceeding from dorsal to ventral (Fig. 5). Because landmark C was on the horizontal septum, line segments AB and BC represent epaxial portions of the myomere whereas line segments CD and DE are the hypaxial portions.

In addition, we performed some destructive dissections of selected myomeres to reveal the anteriorly and posteriorly directed muscle cones.

Figure 5 illustrates 14 morphological variables that we used to describe the arrangement of the four line segments representing a single myoseptum. The straight-line distances between successive landmarks are denoted by AB, BC, CD, and DE, and the angles between each of these line segments and the longitudinal axis will be referred to as ABL, BCL, CDL, and DEL, respectively. To examine the extent to which mirror image (about horizontal septum) portions of the myomere resembled each other, we calculated four indices of symmetry by subtracting the value of the hypaxial variable from that of the appropriate epaxial variable. For example, the variables ABDE and BCCD equal AB-DE and

TABLE 1. Means (N = 5) and ranges for the basic anatomy of specimens used for myomeric dissections

Species	Standard length (mm)	Trunk vertebrae	Caudal vertebrae	Total vertebrae[1]
Micropterus salmoides	158 (147–168)	13 (13–13)	15 (15–15)	30 (30–30)
Ambloplites rupestris	142 (131–150)	11 (10–11)	16 (15–17)	29 (28–29)
Pomoxis nigromaculatus	139 (110–151)	12 (12–12)	17 (16–17)	31 (30–31)
Lepomis macrochirus	141 (131–167)	10 (10–11)	15 (14–15)	27 (27–27)

[1]The total includes two cervical vertebrae and excludes all of the specialized caudal veretebrae that lacked neural and hemal spines.

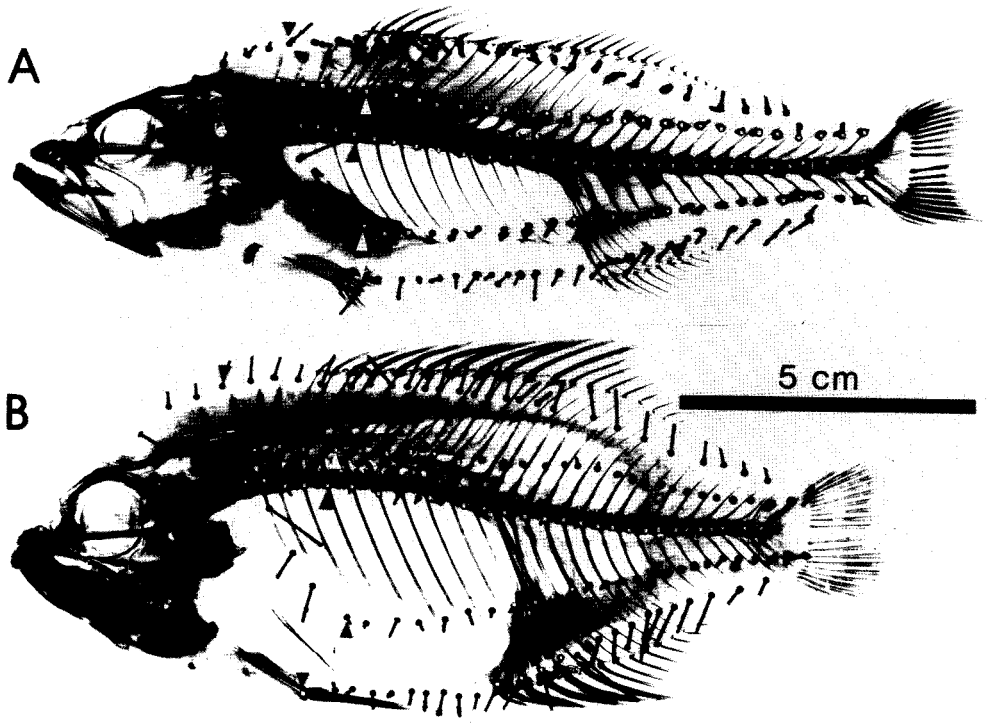

Fig. 1. Photographic prints from lateral-view X-rays used to measure the location of landmarks along the superficial portions of the myosepta: (**A**) *Micropterus salmoides* and (**B**) *Ambloplites rupestris*. The thick horizontal line indicating the distance scale is parallel to the lines used as the longitudinal axes of the fish. The heads (not the stems) of the pins indicate the location of landmarks that were digitized, and for the clarity of illustration, white dots cover some of the pinheads that were obscured on the prints by dense tissue. The white and black triangles point to the landmarks of the most anterior "complete" myoseptum which was counted as number one. This exposure, which most clearly showed the pinheads, did cause some loss of the skeletal details that were apparent in the original X-ray.

BC-CD, respectively. Similarly, ABLDEL and BCLCDL described the symmetry of the angular orientation of different portions of the myomere. We also determined the longitudinal extent (SPAN) and dorsal-ventral distance (HEIGHT) for the entire myomere involving all five landmarks.

Nine variables described the morphology of the axial skeleton based on digitized coordinates of the distal tip and base of all neural spines, ribs, and hemal spines and of the anterior and posterior ventral margins of all vertebral centra. Using these coordinates, we calculated the straight-line distances representing the lengths of 1) each neural spine (from the anterior base to the tip), 2) ribs (from head to tip) or hemal spines (from anterior base to tip), and 3) each centrum (projected onto the longitudinal axis). We determined the angles between the longitudinal axis and the line segments representing the neural spines and ribs or hemal spines. For each collective axial skeletal segment (including the neural spine, centrum, and rib or hemal spine), we calculated the longitudinal span and the total height. Two indices of symmetry compared the lengths and the angles of the neural spine to those of the rib or hemal spine.

We wanted specifically to examine whether certain portions of the myomeres were more variable than others, and whether such variability was statistically significant among species or within a species among different longitudinal locations. Thus, rather than treating each reconstructed W-shaped structure as a single unit, we primarily analyzed the individual variables from each of the four por-

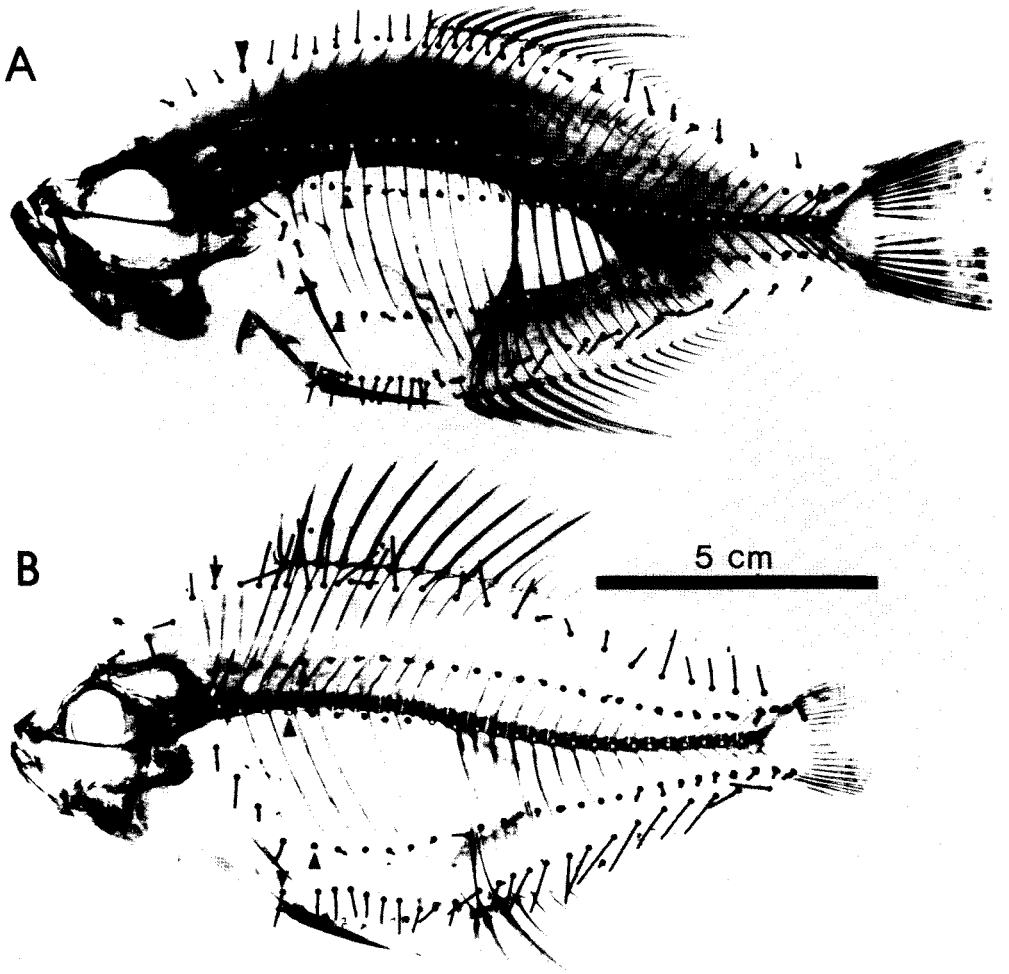

Fig. 2. Photographic prints from lateral-view X-rays used to measure the location of landmarks along the superficial portions of the myosepta: (**A**) *Pomoxis nigromaculatus* and (**B**) *Lepomis macrochirus*. Labeling and conventions are as in Figure 1.

tions comprising a W-shaped structure (Fig. 4). To avoid the statistical complications of different sample sizes and missing cells in our ANOVAs, we excluded the most anterior myomeres which lacked either of the two hypaxial portions that form the ventral portion of the W-shape. We also wanted to correlate myomeric shape with the size of the neural spines and or ribs and hemal spines; therefore, we also excluded some of the axial musculature which was lateral to the most posterior vertebrae and intrinsic tail bones which lacked neural and hemal spines. To reduce the data set further, we chose 11 standardized longitudinal sites including the most anterior and posterior myosepta conforming to the above criteria and nine additional myosepta spaced as near as possible at 10% increments of the number of intervening myosepta (thick lines in Figs. 2 and 3).

Our primary statistical analysis was an ANOVA with species (4 levels) and longitudinal position (11 levels) as fixed crossed factors and individuals (5 levels) as a random factor nested within species. Our analysis focused primarily on the two fixed factors. The F-values of the tests for significant species effects equaled the mean squares (MS) of species divided by the MS of individuals within species (Scheffe, '59). The F-value test-

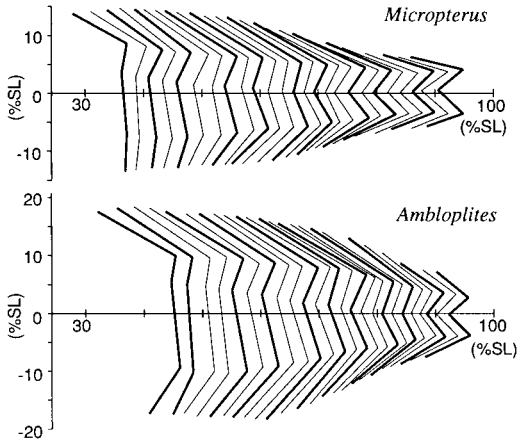

Fig. 3. Lateral view of the schematic reconstruction of the myosepta. Straight lines connect the landmarks within each myoseptum that were digitized from the X-rays, and the thicker lines represent the myosepta used for statistical analysis. The x- and y-axes are to the same scale and indicate distances in % standard length. The x-axis is aligned on the longitudinal axis of each fish and positioned so that 100% is at the posterior edge of the hypural bones. Data are for the same individuals as shown in Figure 1. Only complete myosepta not inserting onto the hypurals at the level of the horizontal septum are shown, whereas in the X-rays some additional pins were often included in the tail region.

ing for the significance of longitudinal position was MS position divided by the MS of position*individual within species. Dividing MS position*species by MS position*individual within species yielded the F-values for the position*species interaction terms which had $P < .005$ for all 23 morphological variables and $P < .001$ for 21 of the 23 ANOVAs. In our experimental design, we were unable to test for the significance of individuals and the position*individual within species interaction term because of the lack of replication within a cell. One rather conservative method used to correct for multiple comparisons is the Bonferroni adjustment, which divides the critical P value by the number of comparisons (.05/23 = ca. .002). As will be presented in more detail in the results, values of P were commonly much less than .001; hence, making this correction was of little consequence for most of our ANOVAs.

Although the mean SL for the taxa studied was similar, there was still some variation in size that could confound interpretation of the ANOVA results. All straight-line distance variables were thus transformed into %SL and these percentages were used in the ANOVA. Hence, all figures of straight-line distance variables also use units of %SL. The mean SL of 14 to 15 cm was chosen to reflect the sizes of fishes used for experimental work on locomotor kinematics and muscle function (Jayne and Lauder, '91, '93, '94). To aid qualitative visualization of the effects of a uniform shape deformation among taxa, figures of reconstructed *Micropterus* myomeres were scaled vertically to match the body depths of other taxa, and these distorted myomeres were superimposed onto the undistorted reconstructed myomeres of the deeper bodied taxa.

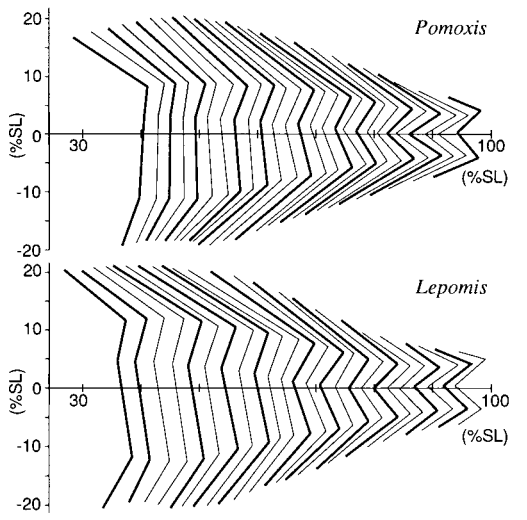

Fig. 4. Left lateral view of the schematic reconstruction of the myosepta. Data are for the same individuals as shown in Figure 2. Conventions are as in Figure 3.

RESULTS

Myomeric morphology

General description

Most of the superficial myomeres schematically conformed to the W-shape which has been described previously by many authors. Notable exceptions to this were the most anterior axial muscles (see landmarks anterior to the triangles in Figs. 1 and 2), which lack some of the ventral portions found in myomeres posterior to the pectoral girdle. This anterior part of the axial musculature is thought to be most important for feeding, and the hypaxial portions of these myomeres increase in size from anterior to posterior up to the level of the pectoral girdle.

The most anterior myoseptum for which landmarks were digitized was noticeably asymmetric (Figs. 1–4), and A was always located more anteriorly than any of the other landmarks regardless of the species. Landmark A of the first complete myoseptum was also generally opposite the first or second

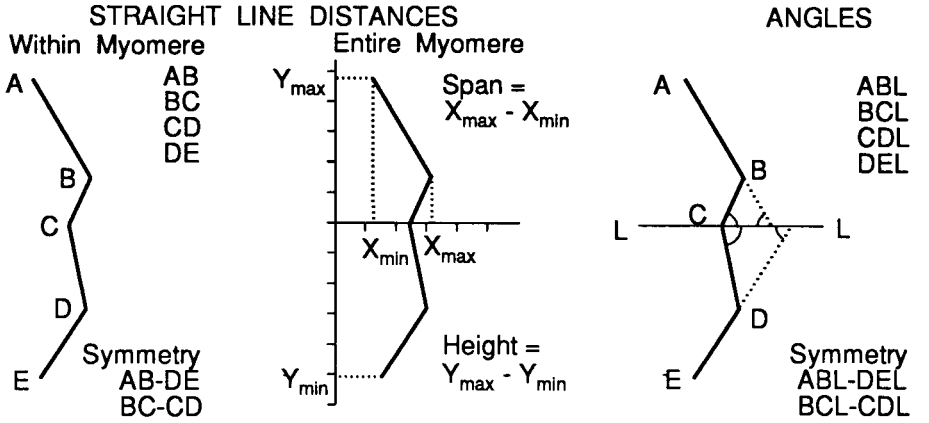

Fig. 5. Measurement scheme used for quantifying myomeric anatomy. A hypothetical schematic myoseptum (as reconstructed in Figs. 3 and 4) is shown oriented so that anterior is to the left. From dorsal to ventral, the landmarks were labeled **A–E,** respectively, and landmark C was on the horizontal septum. Within each myoseptum, the straight-line distances were calculated between adjacent landmarks. The longitudinal span of an entire myoseptum equaled the difference between the minimum and maximum x coordinates from any portion of the myoseptum, and the total height was calculated similarly using the y coordinates. The orientation of each portion of the myoseptum was measured as its angle relative to the longitudinal axis of the fish (L). Indices of epaxial-hypaxial symmetry were calculated as the differences between quantities from portions of the myoseptum that were mirror images about the horizontal septum.

(cervical) vertebrae (Figs. 1, 2). Dissections in the anterior regions of one individual of each species confirmed that the tip of the deep cone extending anteriorly from point C of the first complete myoseptum was always positioned posterior to point A. This deep anterior cone generally ended at the same longitudinal location as landmark E of the first complete myoseptum.

At the level of the horizontal septum (C), the superficial portion of the myomere, visible between adjacent myosepta, spanned approximately one vertebra. However, deep cones of the myomeric musculature extended medially from landmarks B and D and generally projected posteriorly for two (or occasionally three) vertebrae. Thus, the superficial landmarks of a single myoseptum included the most anterior extent of a single myomere, whereas the most posterior superficial landmark of a myoseptum underestimates the most posterior extent of the entire myomere by about three vertebrae. Because of the destructive nature of the dissections required to expose the deeper portions of the myomere, it was not practical to quantify both the superficial and deep morphology of all of the longitudinal sites for all individuals. Hence, the superficial landmarks that we used out of practical necessity allowed us to quantify only part of the shape of the myomere. We further simplified the analysis by working with a two-dimensional lateral projection of the landmarks (Figs. 1, 2), and by approximating the slightly curved myosepta with straight-line measurements (Figs. 3, 4).

Landmark C on the horizontal septum was lateral to the centra of the caudal vertebrae in all four of the centrarchid species that we examined. In at least a part of the trunk region in the deeper-bodied taxa (Figs. 1B; 2A,B) landmark C was commonly ventral to the centra of the underlying vertebrae; this feature was especially pronounced in *Pomoxis* (Fig. 2A). In the trunk, small secondary ribs were usually embedded in the myosepta and terminated slightly deep to landmark C. In contrast to the other three taxa, significant portions of these secondary ribs in *Pomoxis* were often exposed superficially (after the removal of the skin).

Beyond these gross generalizations, it becomes useful to examine the individual morphological variables that describe the myomeric shape among different longitudinal sites and species. Analysis of variance revealed that all 14 of the myomeric variables (Fig. 5) had highly significant variation ($P < .001$; df = 10, 160) attributable to longitudinal position, with F-values ranging from 22 to 821. Thirteen of the 14 myomeric shape variables varied significantly ($P < .05$) among species. Ten of these variables had highly significant variation ($P < .001$) among species, and eight F-values (df = 3, 16) ranged from 19 to 56. In light of the overwhelmingly significant differences among species and longitudinal positions, much of the variation is

best understood by examining the mean values (N = 5) of variables calculated for each species at each longitudinal site (N = 11).

Straight-line distances

The four straight-line distances between adjacent markers showed three different overall patterns of variation among the longitudinal positions (Fig. 6). Both AB and DE varied considerably with longitudinal position, with maximal values of all species occurring at sites roughly midway between the most anterior and posterior locations (Fig. 6A,D). Compared to other portions of the myomere, the length of BC showed only slight longitudinal variation (Fig. 6B) even though this variation among sites was highly significant ($F = 33$, $df = 10, 160$). For all species, maximal values of CD were anterior, and CD declined sharply at progressively more posterior locations until, for the posterior two-thirds of the caudal vertebral column, values were nearly constant among the remaining longitudinal locations.

For all four portions of the myomeres (AB, BC, CD, and DE), *Micropterus* consistently had the smallest values for nearly all of the longitudinal locations (Fig. 6). For portions AB, BC, and CD, *Lepomis* consistently had greater values in the anterior regions compared to any other taxon. Interestingly, *Pomoxis* generally had the greatest values of DE for most longitudinal locations (Fig. 6D), and *Pomoxis* also had the greatest values of AB for the posterior longitudinal locations (Fig. 6E).

For all species, the length of the most dorsal (AB) portion was always greater than or equal to that of the most ventral (DE) portion of the myomere (Fig. 6C). In contrast, for the portions nearest the horizontal septum, the epaxial (BC) portion was usually shorter than the hypaxial (CD) portion (Fig. 6F). For most of the posterior half of the fish, BCCD was nearly zero, indicating a greater extent of symmetry than for the comparison of AB and DE (Fig. 6C). *Micropterus* generally showed least disparity in length between BC and CD (Fig. 6F), whereas for both comparisons of epaxial and hypaxial lengths, *Lepomis* generally had the greatest difference in lengths (Figs. 6C,D).

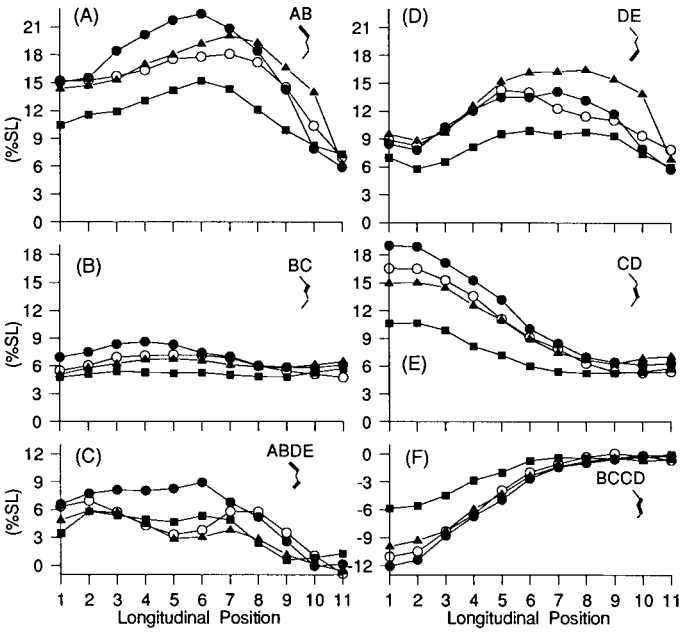

Fig. 6. Mean species values of straight-line distances between myoseptal landmarks for *Micropterus salmoides* (solid squares), *Ambloplites rupestris* (open circles), *Pomoxis nigromaculatus* (solid triangles), and *Lepomis macrochirus* (solid circles). Below each variable name at the upper right of each panel the thick lines schematically indicate the portion of the myomere used to calculate the variable. Values are shown for the epaxial (**A,B**) and hypaxial (**D,E**) portions of the myosepta. Indices of symmetry (**C,F**) are the differences between the epaxial and hypaxial portions which are mirror images about the horizontal septum. The locations of the longitudinal positions are shown in Figures 3–4, and the myoseptum with landmark C lateral to the first caudal vertebrae is between longitudinal positions 5 and 6.

The overall HEIGHT of myomeres was relatively constant in the trunk region of all four centrarchid taxa (Fig. 7A), and HEIGHT declined from the end of the trunk to the most posterior caudal region. In the trunk, *Lepomis* and *Micropterus* had the greatest (44.8% SL) and lowest (27.3% SL) maximal values of HEIGHT, respectively. These interspecific differences in HEIGHT of the myomeres decreased posteriorly to the lowest values at the most posterior location where HEIGHT ranged from 11.8 to 15.6% SL.

The longitudinal SPAN of the five landmarks within a myomere generally had maximal values at intermediate longitudinal locations (Fig. 7B). Similar to the HEIGHT of the myomere, SPAN of the myomere was usually greatest in *Lepomis* and least in *Micropterus,* but in the most posterior locations (positions 7–11) *Pomoxis* had the greatest values of SPAN. At a particular longitudinal location, HEIGHT was commonly more than twice as large as SPAN, and because of different overall myomeric sizes, these differences between HEIGHT and SPAN corresponded to only 5–8% SL posteriorly compared to 19–30% SL anteriorly (Fig. 7A,B). Even when SPAN was expressed in numbers of vertebrae (Fig. 7C) rather than percent SL, this quantity showed considerable longitudinal variation within all of the taxa. Allowing for three vertebrae spanned by the deeper positions of the myomere (not shown in Fig. 7C), as many as ten vertebrae may underlie the combined deep and superficial portions of an entire myomere. Considering that the number of vertebrae in centrarchids approximates 30 (Table 1), the SPAN of an individual myomere represents a considerable fraction of both the length and number of body segments of the fish.

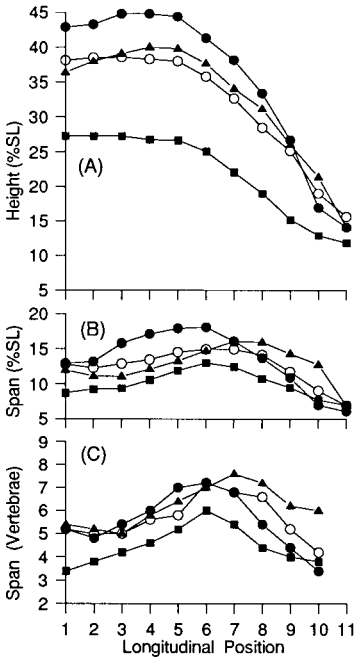

Fig. 7. Mean species values of entire myosepta (all five landmarks) for *Micropterus salmoides* (solid squares), *Ambloplites rupestris* (open circles), *Pomoxis nigromaculatus* (solid triangles), and *Lepomis macrochirus* (solid circles). Height (**A**) is the dorsal-ventral distance. Span is the longitudinal distance expressed as either % standard length (**B**) or as numbers of vertebrae (**C**). Longitudinal positions are as in Figure 6.

Figure 8 shows the extent to which individual portions of the myomere contributed to the overall height of the myomere. For the most posterior location of all species, each portion of the myomere contributed roughly equal amounts to overall myomeric HEIGHT. Portion BC (Fig. 8B) showed only slight longitudinal variation for the anterior seven longitudinal positions, and for all four species, it contributed to less than 21% of HEIGHT at these locations. Portion CD (Fig. 8D) of the myomere was most variable in its contribution to myomeric HEIGHT, ranging from 44% at the most anterior location to less than 20% of HEIGHT at the ninth longitudinal position. Portions AB (Fig. 8A) and DE (Fig. 8C) both generally contributed maximally to overall HEIGHT between longitudinal positions eight and nine. Few conspicuous interspecific trends were apparent for the contribution of the different myomeric portions to overall HEIGHT.

Angles

Figure 9 summarizes the angular orientation of the different portions of the myomere with respect to the longitudinal axis of the fish. BCL and CDL were nearly always acute angles that were directed posteriorly, and ABL and DEL were always acute angles that were oriented anteriorly. For all four species, ABL (Fig. 9A) was usually between 30° and 40°, with the notable exception of the posterior positions within *Micropterus* which had smaller values. The remaining three portions of the myomere all had the largest angles at the first longitudinal position and values decreased posteriorly. The most posterior values of BCL (Fig. 9C) and CDL (Fig. 9E) ranged from 36° to 52° among the four species, whereas those of DEL ranged from 20° to 30°.

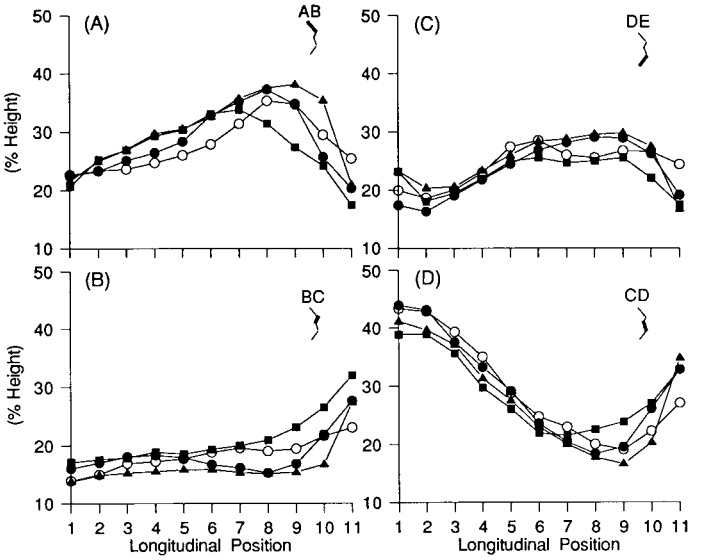

Fig. 8. Mean species values of the relative contribution of different portions of the myoseptum to its overall height for *Micropterus salmoides* (solid squares), *Ambloplites rupestris* (open circles), *Pomoxis nigromaculatus* (solid triangles) and *Lepomis macrochirus* (solid circles). All values for the epaxial (**A,B**) and hypaxial (**C,D**) portions are expressed as the percentage of the height of the myoseptum containing them. Longitudinal positions are as in Figure 6.

For all species, angles of the hypaxial portions of the myomere usually exceeded the values of the mirror image epaxial portion (Fig. 9). The greatest disparity between ABL and DEL (Fig. 9C) occurred anteriorly, and these two angles became more similar posteriorly. For most longitudinal positions, *Pomoxis* had the smallest difference between ABL and DEL (Fig. 9C). For three species, the difference between BCL and CDL was greatest between the second and fourth longitudinal positions, and this difference diminished posteriorly until, at position 7, BCLCDL was close to zero and changed little at increasingly posterior locations (Fig. 9F). In contrast to the other three taxa, BCLCDL of *Lepomis* was nearest zero at the first longitudinal position and tended to decrease posteriorly.

Axial skeleton

Similar to myomeric morphology, all of the nine variables describing the morphology of the axial skeleton had highly significant ($P < .001$) variation attributable to longitudinal position with one F-value equal to 9.2 (centrum length) and the remaining F-values (df = 10, 160) ranging from 56 to 301. All of the nine axial skeleton variables also had significant among-species variation ($P < .05$). Except for two variables (angular symmetry, Fig. 10F; span, Fig. 11C), the among-species variation was highly significant with F-values ranging from 15 to 31 (df = 3, 16).

The mean values for each variable describing the axial skeleton are shown in Figures 10 and 11. The lengths of the neural spines were less than 12% SL for all species (Fig. 10A). *Lepomis* and *Ambloplites* had extremely similar neural spine lengths which were greatest at the sixth longitudinal position. *Micropterus* generally had the shortest neural spines of all the taxa, and the lengths of the neural spines in this species showed an overall decrease posteriorly.

The ribs of all taxa (Fig. 10D) were longest at an intermediate longitudinal location within the trunk for all four taxa. *Lepomis* had some ribs slightly longer than 25% SL whereas *Micropterus* consistently had the shortest ribs, with lengths never exceeding 15% SL. The length of the hemal spines of the vertebrae of all species decreased posteriorly, and mean values for this variable were extremely similar for *Lepomis, Ambloplites,* and *Pomoxis* whereas *Micropterus* had significantly shorter hemal spines (Fig. 10D, positions 7–11).

In all species the length of the neural spine was usually exceeded by that of the rib or

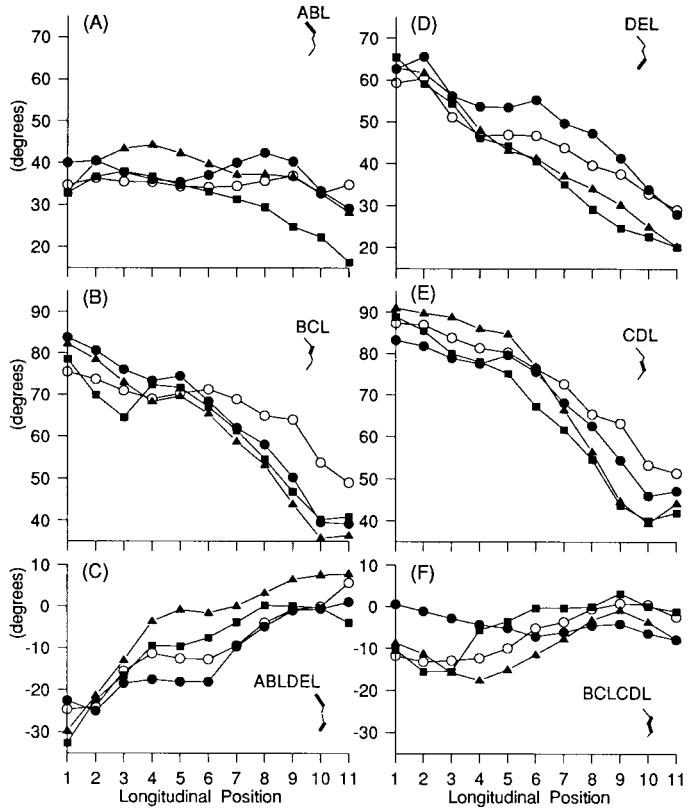

Fig. 9. Mean species values of the angular orientation of the different portions of the myoseptum relative to the longitudinal axis for *Micropterus salmoides* (solid squares), *Ambloplites rupestris* (open circles), *Pomoxis nigromaculatus* (solid triangles), and *Lepomis macrochirus* (solid circles). Figure 5 shows the conventions for determining the angles of the epaxial (**A,B**) and hypaxial (**D,E**) portions relative to the longitudinal axis. The indices of symmetry (**C,F**) are calculated similarly to those in Figure 6. Longitudinal positions are as in Figure 6.

hemal spine on the same vertebrae (Fig. 10C). This difference in length between the dorsal and ventral elements of the axial skeleton was largest at longitudinal positions 3 or 4 for three of the taxa, whereas *Micropterus* tended to have fairly uniform values along the entire length of the trunk. For all four taxa, the difference between the lengths of the neural and hemal spines diminished posteriorly until, at the most posterior location, the lengths of these two structures were nearly identical.

For all species, the angle between the neural spine and the longitudinal axis had a local minimum (was most acute) at an intermediate trunk location (Fig. 10B). Proceeding posteriorly within the caudal vertebrae of all species, the neural spines were progressively more acute relative to the longitudinal axis (Fig. 10B, positions 7–11). For all four species combined, the angle of the ribs did not show a consistent pattern of anterior-posterior change within the trunk. However, the hemal spine angle of all species had a substantial decrease posteriorly within the caudal vertebrae (Fig. 10E).

In all species, the ribs were more nearly perpendicular to the longitudinal axis (horizontal plane) than the neural spines of the corresponding vertebrae (Fig. 10F). Furthermore, the greatest discrepancies between the angles of the ribs and the neural spines (Fig. 10F) tended to occur at the same location as did the greatest discrepancies in the lengths of these two structures (Fig. 10C). In addition, the differences between the angles of the neural and hemal spines of the caudal vertebrae decreased posteriorly until, at the

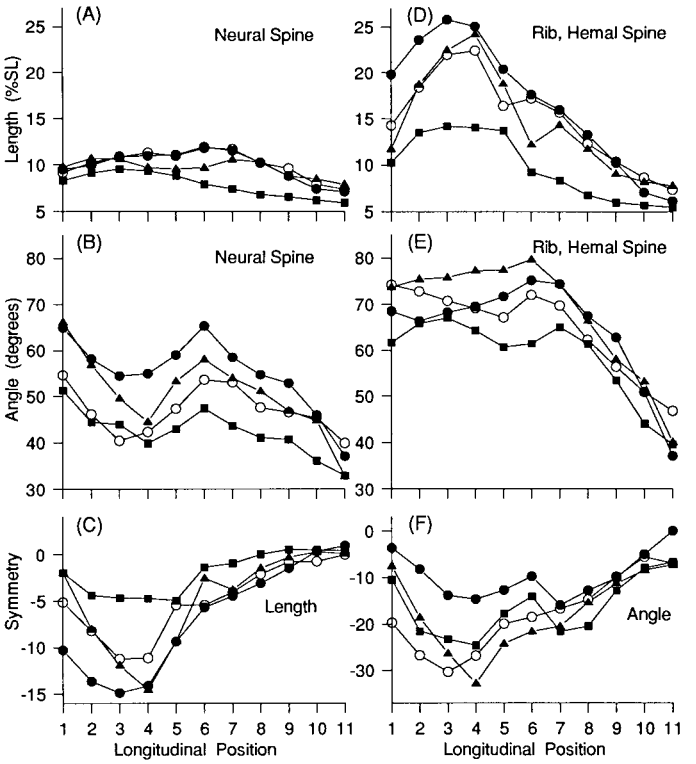

Fig. 10. Mean species values for the axial skeleton of *Micropterus salmoides* (solid squares), *Ambloplites rupestris* (open circles), *Pomoxis nigromaculatus* (solid triangles), and *Lepomis macrochirus* (solid circles). The straight line distances (**A,D**) and angular orientations relative to the longitudinal axis (**B,E**) are shown for both the neural spine of each vertebra and its rib or hemal spine. Indices of symmetry subtracted the length (**C**) or angle (**F**) of the ventral measurement from that of the neural spine. Longitudinal positions are as in Figure 6.

most posterior location, the two quantities were nearly equal.

The centra of the trunk vertebrae were generally longest at an intermediate longitudinal position (Fig. 11A). *Lepomis* consistently had the longest centra at all longitudinal locations, and *Pomoxis* generally had the shortest centra in the trunk. Within the caudal vertebrae *Lepomis* also had the longest centra at an intermediate longitudinal position, but the other taxa showed few consistent trends in change with different longitudinal locations within the caudal vertebrae.

The overall height of the collective segments of the axial skeleton was greatest in all species at an intermediate longitudinal location within the trunk (Fig. 11B), and from this location the height of skeletal segments generally decreased posteriorly. *Micropterus* consistently had the smallest heights of the combined axial skeleton segments, but the difference in height between *Micropterus* and the other species diminished posteriorly.

The longitudinal span of the segments of the axial skeleton was greatest for all species at an intermediate location within the trunk (Fig. 11C). In *Lepomis,* the maximal longitudinal span of the vertebrae and associated structures was 9.5% SL, and this value exceeded that of any other taxon. In the posterior trunk and anterior caudal region, *Pomoxis* had the greatest span of segments of the axial skeleton. Both *Pomoxis* and *Lepomis* had minimal span of the axial skeletal segments in the transitional region between the trunk and the caudal vertebrae. Within each species there was only relatively minor variation in the span of the axial skeletal segments among the different longitudinal positions.

Correlated skeletal and myomeric shapes

Given the highly significant variation in the morphology of both the myomeres and axial skeleton, it is of interest to examine correlations between the morphology of the

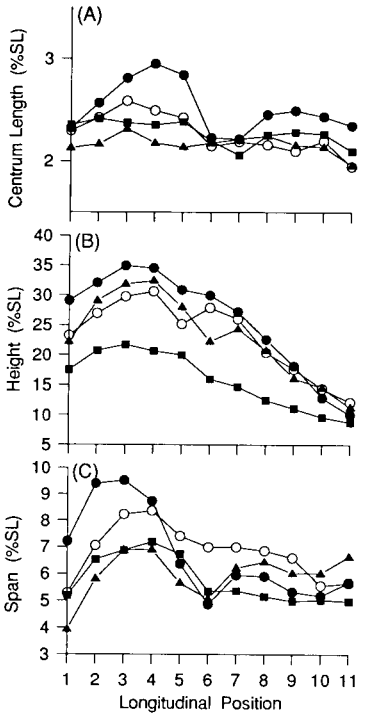

Fig. 11. Mean species values for the axial skeleton of *Micropterus salmoides* (solid squares), *Ambloplites rupestris* (open circles), *Pomoxis nigromaculatus* (solid triangles), and *Lepomis macrochirus* (solid circles). The lengths of the individual vertebral centra (**A**) were measured along the longitudinal axis. The overall height (**B**) was the dorsal ventral distance from the tip of the neural spine to that of the rib or hemal spine of the trunk and caudal vertebrae, respectively. Span (**C**) was the longitudinal distance from the anterior edge of the centrum to the most posterior dimension of either the neural or hemal spine or rib. Longitudinal positions are as in Figure 6.

superficial myomere and the underlying skeleton (Figs. 12, 13). Within a single species, the myomeric variables often had no significant correlation with the axial skeleton, or a pair of morphological variables could vary in a complex fashion from anterior to posterior within a single species. For example, in *Micropterus* the two greatest values of BC occurred for longitudinal positions that had the smallest values of neural spine length, and at the remaining longitudinal sites BC varied minimally while neural spine length increased approximately 50% (Fig. 12A). Within each species, plots of CD versus the lengths of the ribs and hemal spines tended to form a comma-shaped pattern with the bottom of the "comma" being the most posterior site and the upper right of the "comma" indicating positions near mid-trunk.

However, when the species means (four values at each of 11 sites) were considered collectively (N = 44), pairs of morphological variables almost always had highly significant positive correlations. For example, the four comparisons shown in Figure 12 of myomeric and skeletal variables all had highly significant correlation coefficients which ranged from 0.62 to 0.81. One difference between portions BC (Fig. 12D) and CD (Fig. 12B) was that for similar myomeric angular orientations, greater axial skeleton angles (rib/hemal spine) were often associated with CD.

Figure 13 shows the correlations between the overall heights and spans of the myomere (excluding the deep portions) and axial skeletal segments (including the neural spines, ribs, and hemal spines). For all 44 data points, there were highly significant positive correlations between HEIGHT and SPAN of the myomere (Fig. 13A, $r = 0.78$) and between HEIGHT and SPAN of the skeletal segments (Fig. 13C, $r = 0.63$). The closest association between any myomeric and skeletal variable occurred between the HEIGHT of the myomere and the HEIGHT of the skeletal segment (Fig. 13B, $r = 0.96$), and unlike many of the other paired comparisons of morphological variables, the heights of the myomere and skeletal segments also had clear positive correlations within each of the four species.

In contrast to HEIGHT, SPAN of the myomere was only weakly correlated with SPAN of the axial skeleton (Fig. 13D, $r = 0.34$, $P = .02$), and if a correction were made for multiple comparisons this would not be considered significant. HEIGHT of the axial skeleton generally exceeded two-thirds of the HEIGHT of the myomere (mean = 72%, range = 59–82%, SD = 6.0%, N = 44) and this ratio showed no clear trend in longitudinal variation within each species. In contrast, the SPAN of the axial skeleton ranged widely from 27% to 95% of the SPAN of superficial myoseptal landmarks (mean = 55%, SD = 15%), and within each species, maximal and minimal values of skeletal SPAN divided by myomeric SPAN always occurred at the most posterior position and the position between the trunk and tail, respectively. Hence, it is intriguing that HEIGHT and SPAN of the myomere compared to the skeleton showed such striking differences.

Patterns of variance

The previous results dealt primarily with comparisons of mean values, but it is also

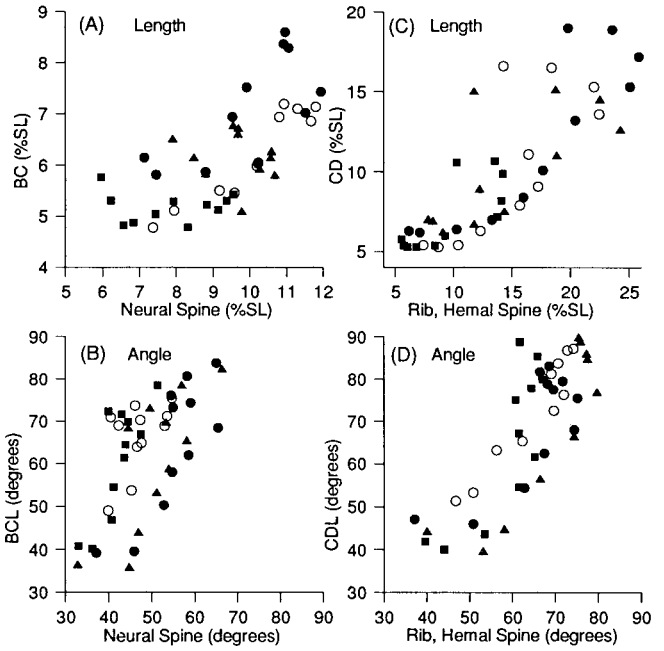

Fig. 12. Mean species values for pairs of variables describing the morphology of myomeres and underlying segments of the axial skeleton of *Micropterus salmoides* (solid squares), *Ambloplites rupestris* (open circles), *Pomoxis nigromaculatus* (solid triangles), and *Lepomis macrochirus* (solid circles). Length (**A**) and angle (**B**) of myomeric portion BC versus that of the neural spine. Length (**C**) and angle (**D**) of myomeric portion CD versus that of the rib or hemal spine. Correlation coefficients (N = 44) of panels A through D were 0.68, 0.62, 0.77, and 0.81, respectively.

useful to compare the variance of different morphological variables. For example, our ANOVAs could detect whether a particular variable differed significantly among species or among longitudinal positions, but such an analysis would not indicate whether one species had greater longitudinal diversity in morphology compared to another species. Furthermore, only analyzing means does not readily indicate if certain aspects of morphology are more variable than others.

Table 2 lists the variance among the 11 longitudinal positions calculated from the means of all five individuals that were measured within each species. For all eight of the myomere variables derived from straight-line distances (Table 2, top 4 rows), *Micropterus* always had the lowest variance among the longitudinal positions compared to those values for the other three taxa. In other words, the linear dimensions of the myomeres of *Micropterus* showed the least variability along the length of the fish. In contrast, for seven of the eight linear distances of the myomeres, *Lepomis* had the greatest longitudinal variation. The variance of DE among the longitudinal positions within *Pomoxis* was more than twice that of both *Lepomis* and *Pomoxis,* but no other trends clearly differentiated *Pomoxis* from *Ambloplites,* which usually had similar, intermediate (to *Micropterus* and *Lepomis*) values of longitudinal variance for the straight-line distances (Table 2).

In light of the minimal longitudinal variation in the myomeric distances of *Micropterus,* one might expect similar uniformity in this species for other myomeric measurements, but this was definitely not the case. For example, the angular orientation of the most dorsal portion of the myomere (ABL) of *Micropterus* had nearly twice the variance among longitudinal positions (46.3 versus 24.6) compared to the next highest species (*Pomoxis*), and the variance within *Lepomis* was only about one-sixth of that in *Micropterus* (Table 2). Furthermore, when the taxa are ranked by the magnitude of the longitudinal variance, different rank orders occur for the distance and angular variables (e.g., see

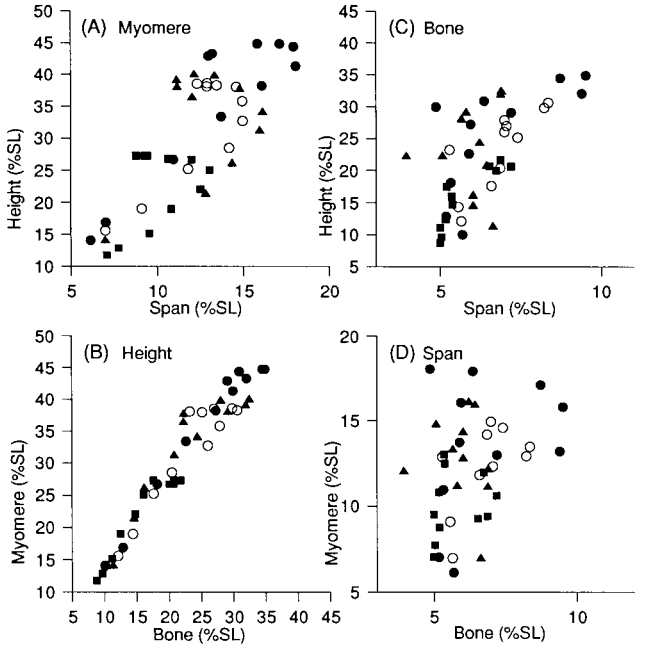

Fig. 13. Mean species values for pairs of variables describing the overall vertical (height) and longitudinal (span) dimensions of myomeres and underlying segments of the axial skeleton of *Micropterus salmoides* (solid squares), *Ambloplites rupestris* (open circles), *Pomoxis nigromaculatus* (solid triangles), and *Lepomis macrochirus* (solid circles). Height of the myomere versus span of the myomere (**A**) and span of the axial skeletal segment (**B**). Height of the axial skeletal segment versus its span (**C**) and span of the myomere versus that of the axial skeletal segment (**D**). Correlation coefficients (N = 44) of panels A through D were 0.78, 0.96, 0.63, and 0.34, respectively.

BC versus BCL in Table 2). Hence, the angular measurements and the linear distances did not show similar patterns of conservatism longitudinally within each of the four taxa.

Table 3 lists values of variance calculated separately for each of the longitudinal positions using the four mean values of each of the species. Thus, high values of this quantity indicate more diverse morphology among species. The among-species variance did not show similar trends with longitudinal position for all four of the within-myomere distances (AB, BC, CD, and DE). For example, the among-species variance in CD declined steadily from anterior to posterior (Table 3) and BC showed a similar trend although it was not as conspicuous. In contrast, the greatest variance among species for AB and DE occurred at the eighth longitudinal position,

TABLE 2. Longitudinal variance in myomeric morphology within each of the four species

	Myomeric variable							
Taxon	AB	BC	CD	DE	ABDE	BCCD	Height	Span
Micropterus	6.43	0.08	4.92	2.54	3.93	5.09	38.26	3.67
Ambloplites	11.77	0.80	21.00	4.84	5.69	18.53	71.13	6.31
Pomoxis	14.74	0.24	13.02	12.31	4.60	14.06	74.06	6.82
Lepomis	19.45	1.09	26.91	6.06	8.29	20.47	87.80	12.04

	ABL	BCL	CDL	DEL	ABLDEL	BCLCDL
Micropterus	46.3	175.6	321.5	234.1	108.5	42.7
Ambloplites	1.3	67.6	165.7	97.0	92.3	32.5
Pomoxis	24.6	264.6	413.8	205.1	151.3	30.4
Lepomis	8.0	197.8	160.9	88.4	78.8	5.8

TABLE 3. Among-species variance in myomeric morphology at each of the longitudinal sites

Longitudinal site	Myomeric variable							
	AB	BC	CD	DE	ABDE	BCCD	Height	Span
1	5.04	0.90	12.35	1.17	2.09	7.42	43.2	3.92
2	3.33	1.02	11.96	1.76	0.86	6.57	46.4	2.89
3	7.07	1.56	9.55	3.02	1.61	4.06	54.5	7.51
4	8.38	1.84	9.28	4.28	3.10	3.20	59.2	7.71
5	9.53	1.61	6.23	6.21	5.94	1.59	57.1	6.49
6	9.10	0.89	3.08	6.88	6.86	0.72	48.2	4.39
7	8.44	0.81	1.74	8.21	1.59	0.23	46.5	2.89
8	10.32	0.31	0.56	8.27	2.84	0.09	41.0	4.57
9	7.99	0.23	0.34	6.70	1.76	0.07	29.7	4.11
10	7.89	0.22	0.52	8.70	0.28	0.07	13.3	6.61
11	0.41	0.55	0.50	0.90	0.94	0.08	2.5	0.18
	ABL	BCL	CDL	DEL	ABLDEL	BCLCDL		
1	10.7	14.0	10.9	6.4	21.1	31.0		
2	5.1	23.2	10.9	7.7	2.5	40.0		
3	11.2	24.2	20.0	6.1	5.4	37.1		
4	17.5	6.1	15.4	11.5	33.0	39.3		
5	14.2	4.5	15.3	21.8	52.6	27.4		
6	9.2	6.1	20.5	45.3	49.5	21.5		
7	13.8	18.8	20.3	44.1	22.5	10.2		
8	29.3	27.2	25.7	60.6	14.0	4.5		
9	45.9	78.2	83.7	55.0	12.4	9.3		
10	28.0	61.9	41.6	31.0	15.7	10.9		
11	59.8	29.6	16.3	23.2	27.3	12.9		

and for these two variables the relative increases in the among-species variance were not as large as that of CD.

One index of linear symmetry, BCCD, showed a regular and large posterior decrease in its among-species variance (Table 3), but ABDE did not have such a pattern. The among-species variance in overall HEIGHT of the myomere was remarkably similar for the most anterior eight longitudinal positions, and then it declined considerably for the most posterior three sites. In contrast, the overall SPAN of the myomere showed few consistent trends in among-species variance for different longitudinal positions.

The among-species variance in the myomeric angular orientations showed little regular change among the longitudinal sites (Table 3). BCL tended to be least variable among species at intermediate longitudinal positions, and DEL was least variable among species at the most anterior three longitudinal positions.

When comparing the variances shown in Tables 2 and 3, the most obvious trend was that BC usually had the smallest values of variance both among species (Table 3) and among different longitudinal locations within a species (Table 3). Hence, BC was the most conservative feature of the myomeric morphology which we quantified. CD and AB both represented the other extreme by having large longitudinal variability within a species (Table 2) as well as having some of the greatest variability among species (Table 3, but at different longitudinal positions). Overall HEIGHT of the myomere consistently had both a greater among-species variance and greater longitudinal variance compared to the similar values for overall SPAN of the myomere.

DISCUSSION

We deliberately chose four species of fishes with different external shapes which are presumed to be relevant to the performance of different locomotor tasks (Webb, '84), and we sought to determine how various aspects of internal morphology correlated with variation in external height along the body in each species. We will consider three of many potential alternatives by which the myomeric shape could be deformed to attain greater overall height. 1) All four parts of the myomere could enlarge proportionally. Such enlargement would preserve the angles ABL, BCL, CDL, and DEL, and the longitudinal span of these myomeres with greater height would necessarily also be larger. 2) Each of the myomeric portions could be oriented more nearly perpendicular to the horizontal (fron-

tal) plane of the fish. If the lengths of the myomeric portions were not simultaneously increased, this mechanism would necessarily decrease the longitudinal span. 3) Myomeres could be "stretched" vertically while preserving the longitudinal dimensions (Fig. 14), and this would also result in more nearly perpendicular orientations of the myomeric portions relative to the horizontal plane. Because variation in height occurs within the body of individual fish as well as among the different species of centrarchids, we also wanted to determine whether or not the anterior increase in myomeric height occurred in a fashion similar to the conspicuous increases in height found among the four species.

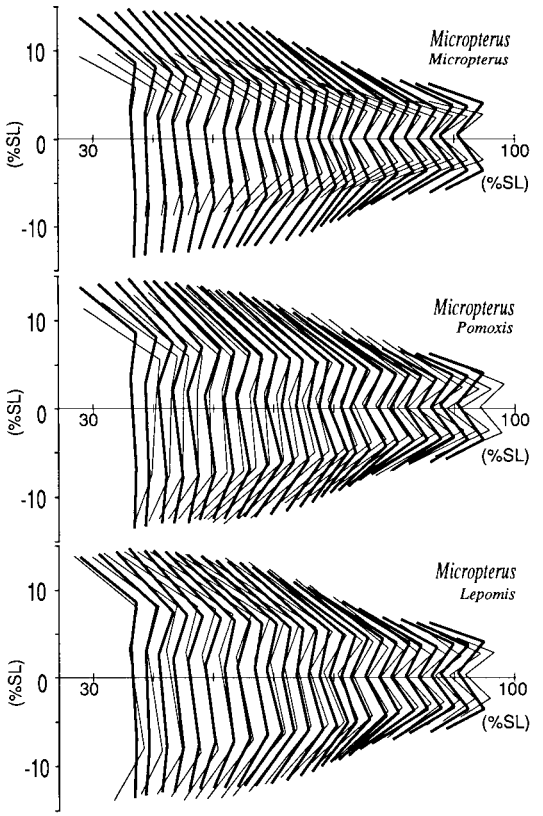

Fig. 14. Illustration of overall shape differences among taxa in myomere morphology. In each panel, to match the body depth of *Lepomis macrochirus* and *Pomoxis nigromaculatus*, the myomeric shape of *Micropterus salmoides* (bold lines) has been elongated to 148% of its original size in the y-dimension only, and overlain on the taxon indicated (whose undistorted myomeres are shown in thin lines). The y-axis indicates the scale for only the elongated myomeres.

For the four most posterior positions (8–11), the overall height of the myomeres nearly doubled from posterior to anterior (Fig. 7A). In this posterior region, the angles of all four parts of the myomere also increased anteriorly (Fig. 9A,B,D,E). Although the lengths of BC and CD were nearly invariant in this region (Fig. 6B,C), the lengths of both AB and DE (Fig. 6A,D) increased anteriorly. Hence, these anteriorly directed increases in myomeric height in the caudal region involved a combination of alternatives 1 and 2 while these myomeres (positions 8–11) fundamentally retained their linear (Fig. 6C,F) and angular (Fig. 9C,F) symmetry. The increase in longitudinal span from position 11 to 8 does not conform to the morphology predicted from vertical "stretching." At position 11 the overall myomeric heights (Fig. 7A) and the lengths of each part of the myomere (Fig. 6A,B,D,E) were nearly indistinguishable among the four taxa. The cumulative longitudinal changes in myomeric shape resulted in *Ambloplites, Pomoxis* and *Lepomis* being well differentiated from *Micropterus* by the eighth longitudinal position, but these three deeper-bodied taxa still had very similar myomeric heights at this location.

More anterior (longitudinal positions 1–7) increases in myomeric height both among species and anteriorly within each species generally resulted from changes (inconsistent with alternative 1) which preserved neither the shape nor the symmetry of the myomere. Instead, the overall increases in myomeric HEIGHT that occurred longitudinally (Fig. 7A) primarily resulted from differences in the morphology of the hypaxial portion of the myomeres nearest the horizontal septum which contributed disproportionately to overall myomeric height (Fig. 8D). Besides CD being longest anteriorly and longest in the deep-bodied species (Fig. 6E), it was also most nearly perpendicular to the horizontal plane (Fig. 9E) in the anterior region of all four species of fish.

Between longitudinal positions 1–5 within each of the species, myomeric height was nearly constant and at its maximal value (Fig. 7A), and compared to more posterior longitudinal positions, the orientations of two myomeric portions in addition to CD were more nearly perpendicular to the horizontal plane (Fig. 9B,D,E). In this most anterior region, the lengths of the most dorsal (AB) and ventral (DE) parts of the myomere actually decreased (Fig. 6A,D). However, a combi-

nation of increased value of angular orientations (Fig. 9B,D,E) and increased length of CD were sufficient to preserve maximal myomere height in the anterior trunk.

Within the centrarchid fishes, *Ambloplites* and *Pomoxis* are members of one major clade, whereas all species of *Lepomis* are in a different major group. *Micropterus* is the sister group to these two combined lineages (see Wainwright and Lauder, '92; Mabee, '93). *Pomoxis* has a relatively deep body compared to *Ambloplites,* and *Lepomis macrochirus* has a relatively deep body compared to the more generalized species *Lepomis cyanellus*. Furthermore, most centrachid genera have relatively deep bodies compared to *Micropterus*. Hence, based on these phylogenetic relationships, it appears that *Micropterus* has the most generalized external body shape (and shares this shape with clades that are outgroups to centrarchids), and the extremely deep bodies found in both *Pomoxis* and several species of *Lepomis* (including *macrochirus*) have evolved independently.

The deepest-bodied taxa in the present study (Figs. 2, 4: *Lepomis* and *Pomoxis*) commonly had increased values of angular orientations within myomeres (Fig. 9) compared to those of the more generalized *Micropterus* at a similar longitudinal position. "Vertical stretching" of the myomeres (alternative 3) is one of the two previous alternatives that would result in such a deformation. Using one alternative to transform the generalized centrachid myomeric shape found in *Micropterus* facilitates visualizing the sufficiency of one explanation to account for the observed interspecific differences in shape.

Figure 14 compares vertically elongated (alternative 3) myomeric shapes of *Micropterus* to their original shape as well as those of the deep-bodied *Lepomis* and *Pomoxis*. It appears that vertical elongation of the myomeric shape could explain much of the observed interspecific variation that is associated with a deep external body shape (Fig. 14). For example, in both *Pomoxis* and *Lepomis* the locations of landmarks B, C, and D are very similar to those of elongated *Micropterus* myomeres as a result of overall similarity in the lengths and orientation of myomeric portions BC and CD. The lengths and orientations of AB in *Pomoxis* and DE in *Lepomis* are also very similar to the predictions from vertical elongation of *Micropterus* myomeres.

Three major discrepancies occur between the vertically elongated myomeres of *Micropterus* and those of the deep-bodied taxa. First, the three most posterior elongated myomeres had an excessive heights as compared to those of both *Pomoxis* and *Lepomis* (Fig. 14). Second, *Pomoxis* consistently had more acute values of DEL than those of the elongated *Micropterus* myomeres. In fact, the orientations of DE in *Pomoxis* were nearly identical with those found in the undistorted myomeres of *Micropterus* (Fig. 9D) whereas the lengths of DE in *Pomoxis* generally exceeded those of *Micropterus* and all other taxa (Fig. 6D). Finally, *Lepomis* consistently had more acute values of ABL than those of the elongated myomeres (Fig. 14). These latter two departures from vertical elongation of *Micropterus* myomeres nicely illustrate how convergent changes in external shape (to a deep body) had some concomitant divergent changes in internal morphology.

In all species, some longitudinal differences in myomeric morphology parallel those observed with increased depth of the body among different species. For example, proceeding anteriorly from the most caudal site, the lengths of most portions of the myomere increase and CD shows an especially large increase. Anteriorly, the orientations of most myomeric elements also become progressively more vertical (perpendicular to the horizontal plane). No single alternative (of the three considered) was sufficient to explain the variable myomeric shape associated with height differences that occur either longitudinally or among different species. However, many of the observed changes associated with deep-bodied condition are consistent with vertical elongation of myomeric shape (alternative 3). If all of the vertical coordinates of the *Micropterus* landmarks increased by the same relative amount (vertical elongation), segment CD would show a much larger absolute difference after such a transformation because of different original size and orientation (longer and more vertical) compared to other parts of the myomere. Hence, even some of the seemingly disproportionate increases in CD found in the deep-bodied taxa (Fig. 6E) are consistent with the notion of vertical elongation of myomeric shape.

It is interesting to consider further the longitudinal and interspecific changes that occur in the symmetry of myomeres. Nursall's ('56) comparisons of the myomeric shape of aquatic chordates found that the superficial

myomeric shape of the lamprey (*Petromyzon*) is fairly symmetric along much of the animal's length although some of the details of the myomeric shape do change longitudinally. Within a shark (*Squalus*) and a teleost fish (*Perca*), the most symmetric myomeric shapes subjectively appear to be posterior to the trunk (Fig. 1 in Nursall, '56). Additional figures of the myomeres in teleost fishes (Greene and Greene, '14; Videler, '75; Wainwright, '83), combined with our findings for centrarchids, support the generalization that the greatest dorsal-ventral symmetry of the myomeres occurs caudally.

It seems likely that the elongate shape and relatively uniform height of *Petromyzon* is probably specialized. Although many early teleost fishes (known only from fossils) are quite deep bodied, many primitive extant actinopterygii such as *Polypterus, Amia* and Lepisosteidae also have minimal longitudinal variation in height. Our preliminary dissections of *Amia* suggest that fairly symmetric myomeres occur within this outgroup for the teleost fishes. It would be interesting if additional studies could determine where in the evolution of chordates there may have been substantial departures from symmetric myomeric musculature. Another interesting question is whether some diverse elongate actinopterygians may have convergently acquired increased myomeric symmetry, or, in the case of certain primitive taxa, might greater myomeric symmetry actually be a retained primitive condition.

Functional implications of axial structure

Much of the diversity in the locomotion of fishes has been categorized by the longitudinal extent of the undulating axial structures (Breder, '26; Lindsey, '78), and it would be useful if the amplitude of lateral undulation had a clear skeletal or myological correlate. However, the angles of the muscle fibers even within a single myomere differ considerably and this complicates prediction of the functional consequences of variability in myomeric shape (Alexander, '69). However, the myosepts (which we used to define landmarks) are the primary site for attachment of the axial muscle fibers, and hence must be an important mechanical link for force transmission.

Perhaps a grossly symmetric myomeric morphology facilitates lateral bending while minimizing torsion and/or dorsal-ventral flexion of the vertebral column. Current literature has examined neither the within-myomere patterns of muscle activation nor the mechanical behaviors of the axial skeleton that are relevant to the issue of potential torsional forces that may occur during the swimming of fish. One major cause of myomeric asymmetry in the centrarchids is enlargement of CD, but a large portion of CD overlaying the distal ribs is quite thin in cross-section compared to the epaxial portion of the myomere at the same longitudinal location. Consequently, these differential amounts of muscle further limit the ability to predict the consequences of the myomeric shape differences.

Although the caudal region of centrarchids and many fish taxa is fundamentally important in the transmission of locomotor forces, muscle activity is not limited to the caudal region of most undulatory swimmers (Grillner and Kashin, '76; Williams et al., '89) including centrarchid fishes (Jayne and Lauder, '91, '93). As muscle activity propagates from head to tail during undulatory swimming, the extent to which all of the contractile tissue within a myomere is activated synchronously is little known. Only Liu and Westerfield ('88) have experimentally addressed this issue for the white myomeric musculature, and they found that there was generally coactivation in the two portions of the myomere nearest the horizontal septum (BC & CD); however, it is not known how portions AB and DE are activated during swimming and whether or not there is heterogeneity in the timing of activation of myomeric portions BC and CD among areas of different depth. Relevant to this issue of coactivation is the recent finding by Jayne and Lauder ('94) that the onset of red muscle activity could occur significantly before that of underlying white muscle at the same longitudinal location within *Lepomis macrochirus* during burst and glide swimming. Myosepta are evident in the superficial muscle of *Lepomis;* therefore, the red muscle might be considered as a very specialized (lateral) portion of the overall myomeric structure. Thus, at least some evidence suggests that it is indeed possible to not have coactivation of all of the contractile tissue comprising an axial muscle segment.

The pattern of muscle activation within a myomere as well as the arrangement of myomeres relative to the axial skeleton suggests the following question: What are the fundamental units of muscle recruitment (parts of myomeres, entire myomeres, or multiple por-

tions of different myomeres) that are involved in the axial undulations of fishes? The pattern of innervation within a myomere is complex and does not itself suggest a clear a priori hypothesis of myomeric function. For example, in the zebra fish, three primary motor units have been identified (Westerfield et al., '86), and their names, based on the location of the cell bodies within the spinal cord, are the rostral (RoP), middle (MiP), and caudal (CaP) primary motoneurons. These three motoneurons each have mutually exclusive territories in the white muscle of the myomere with MiP innervating myomeric portion BC, and RoP and CaP, respectively, innervating the dorsal and ventral parts of myomeric portion CD (Westerfield et al., '86). Disproportionate enlargement of myomeric portion CD characterizes deep-bodied fish such as *Lepomis*. Hence, it would be interesting to determine whether or not the territories of RoP and CaP occupy similar fractions of myomeric portion CD either longitudinally within a fish or among different species of fish when myomeric dimensions differ.

Illustrations of the motor unit territories of RoP, MiP, and CaP (Westerfield et al., '86, Fig. 5) suggest that their longitudinal extent is only about two vertebrae in the zebra fish, and some portions within the myomere (AB & DE) are clearly not covered by the cumulative area of these three territories. Westerfield et al. ('86) did not indicate the longitudinal extent of the entire myomere, and it is not clear whether the most extreme longitudinal positions within a myomere are innervated by any of the primary motoneurons in this species. Secondary motoneurons have territories that may overlap those of the primary motoneurons and, unlike the primary motoneurons, they may innervate more than one myomere and hence overlap with the territory of a motoneuron from a different spinal segment (Westerfield et al., '86). Besides this within-species diversity in muscle innervation, the extent to which muscle fiber innervation is polyneuronal or has multiple terminals varies among different fish taxa (Johnston, '83). Consequently, current neuroanatomical and neurophysiological information is not sufficient to predict whether an entire myomere can or must be activated synchronously and how many spinal segments innervate a single myomere.

A striking finding of our study of the myomeres in centrarchids was that an individual myomere (including deep portions) may span as many ten out a total of 30 body segments. Furthermore, the longitudinal extent of the myomeres was not constant along the length of a single fish either in terms of percent SL or in numbers of body segments (Fig. 7). Consequently, if muscle along the length of the fish were to be activated such that a constant fraction of the fishes length or number of body segments were affected, then for some myomeres the entire myomere necessarily could not be activated synchronously.

The myomeres of centrarchids generally spanned the most vertebrae in the transitional region between the trunk and caudal vertebrae. If entire myomeres were activated synchronously, then it seems likely that the flexibility of fishes and the fineness of control of lateral flexion would decrease as muscular segments spanned greater numbers of body segments. Hence, large myomeres at an intermediate longitudinal location potentially could facilitate stiffening an area that is important for caudally transmitting forces which are generated in the trunk. Although centrarchid species vary minimally in their numbers of vertebrae (Table 1; Mabee, '93), comparisons among phylogentically more diverse taxa reveal that, even for fishes with a generalized body shape, numbers of vertebrae vary considerably. For example, salmonids have between 56 and 75 total vertebrae (Scott and Crossman, '73) while having myomeres that span from ten to 15 body segments (Greene and Greene, '14). Thus, these features of the salmonid morphology might increase axial flexibility and involve a different co-ordination between the activation of muscle and lateral bending compared to centrarchids.

In light of the tremendous complexity in the neuroanatomy and axial morphology of fishes, it is extremely difficult at the present time to make informed predictions about axial function during undulatory swimming. Systematic comparative electromyographic studies of muscle activity during swimming should help to reduce the number of possibilities for neural and mechanical mechanisms underlying swimming. We have recently completed a series of electromyographic experiments on *Lepomis* and *Micropterus* designed to address the effect of different overall body shape between closely related species with similar numbers of body segments. Furthermore, comparing *Micropterus* with the trout (Williams et al., '89) should help to clarify some of the consequences of different numbers of body

segments. Finally, by studying behaviors over a wide range of speeds that require a greater portions of the total musculature to be recruited, insights should be gained into the extent to which entire myomeres are utilized.

ACKNOWLEDGMENTS

We are grateful to S. Weldy at the El Toro Animal Hospital and J. Seigel at the Section of Fishes at the Los Angeles County Museum for the X-rays of specimens. Julian Humphries kindly arranged the loan of centrarchid specimens on which this paper was in part based. Support was provided by NSF grants BNS 8919497 to B.C.J. and G.V.L. and NSF BSR 9007994 to G.V.L. The high-speed video system was obtained under NSF BBS 8820664.

LITERATURE CITED

Alexander, R.M. (1969) The orientation of muscle fibres in the myomeres of fishes. J. Marine Biol. Assoc. UK. *49:*263–290.

Altringham, J.D., C.S. Wardle, and C.I. Smith (1993) Myotomal muscle function at different locations in the body of a swimming fish. J. Exp. Biol. *182:*191–206.

Blight, A.R. (1977) The muscular control of vertebrate swimming movements. Biol. Rev. *52:*181–218.

Bone, Q. (1978) Locomotor muscle. In W.S. Hoar and D.J. Randall (eds): Fish Physiology, Vol. VII. Locomotion. New York: Academic Press, pp. 361–424.

Breder, C.M. (1926) The locomotion of fishes. Zoologica *4:*159–297.

Gibb, A.C., B.C. Jayne, and G.V. Lauder (1994) Kinematics of pectoral fin locomotion in the bluegill sunfish, *Lepomis macrochirus.* J. Exp. Biol. (in press).

Greene, C.W., and C.H. Greene (1914) The skeletal musculature of the king salmon. Bull. Bur. Fish. *33:*25–59.

Grillner, S., and S. Kashin (1976) On the generation and performance of swimming in fish. In R.M. Herman, S. Grillner, P.S.G. Stein, and D.G. Stuart (eds): Neural Control of Locomotion. New York: Plenum Press, pp. 181–201.

Harder, W. (1975) Anatomy of Fishes. Stuttgart: E. Schweizerbart'sche Verlagsbuchhandlung.

Jayne, B.C., and G.V. Lauder (1991) Kinematics and muscle activity of swimming in the largemouth bass. Am. Zool. *31:*95A.

Jayne, B.C., and G.V. Lauder (1993) Red and white muscle activity and kinematics of the escape response of the bluegill sunfish during swimming. J. Comp. Physiol. A. *173:*495–508.

Jayne, B.C., and G.V. Lauder (1994) How swimming fish use slow and fast muscle fibers: implications for models of vertebrate muscle recruitment. J. Comp. Physiol. A. (in press).

Johnston, I.A. (1983) Dynamic properties of fish muscle. In: P.W. Webb and D. Weihs (eds): Fish Biomechanics. New York: Praeger Publishers, pp. 35–67.

Lauder, G.V. and Liem, K.F. (1983) The evolution and interrelationships of the actinopterygian fishes. Bull. Mus. Comp. Zool. *150:*95–197.

Lindsey, C.C. (1978) Form, function, and locomotory habits in fish. In W.S. Hoar, and D.J. Randall (eds): Fish Physiology, Vol. VII. New York: Academic Press, pp. 1–100.

Liu, D.W., and M. Westerfield (1988) Function of identified motoneurones and co-ordination of primary and secondary motor systems during zebra fish swimming. J. Physiol. (Lond.) *403:*73–89.

Long, J.H., Jr. (1992) Stiffness and damping forces in the intervertebral joints of blue marlin (*Makaira nigricans*). J. Exp. Biol. *162:*131–155.

Mabee, P.M. (1993) Phylogenetic interpretation of ontogenetic change: sorting out the actual and artifactual in an empirical case study of centrarchid fishes. Zool. J. Linn. Soc. Lond. *107:*175–291.

Nursall, J.R. (1956) The lateral musculature and the swimming of fish. Proc. Zool. Soc. Lond. *126:*127–143.

Rome, L.C., D. Swank, and D. Corda (1993) How fish power swimming. Science *261:*340–343.

Scheffe, H. (1959) The Analysis of Variance. New York: John Wiley and Sons, Inc.

Scott, W.B., and E.J. Crossman (1973) Freshwater Fishes of Canada. Ottawa: Fisheries Research Board of Canada.

Van Leeuwen, J.L., M.J.M. Lenkheet, and J.W.M. Osse (1990) Function of red axial muscles of carp (*Cyprinus carpio*): recruitment and power output during swimming in different modes. J. Zool. Lond. *220:*123–145.

Videler, J.J. (1975) On the interrelationships between morphology and movement in the tail of the cichlid fish *Tilapia nilotica* (L.). Neth. J. Zool. *25:*143–194.

Wainwright, P.C., and G.V. Lauder (1992) The evolution of feeding biology in sunfishes (Centrarchidae). In R.L. Mayden (ed): Systematics, Historical Ecology, and North American Freshwater Fishes. Stanford: Stanford University Press, pp. 472–491.

Wainwright, S.A. (1983) To bend a fish. In P.W. Webb and D. Weihs (eds): Fish Biomechanics. New York: Praeger Publishers, pp. 68–91.

Waterman, R.E. (1969) Development of the lateral musculature in the teleost, *Brachydanio rerio:* a fine structural study. Am. J. Anat. *125:*457–494.

Webb, P.W. (1975) Hydrodynamics and energetics of fish propulsion. Bull. Fish. Res. Board Can. *190:*1–159.

Webb, P.W. (1978a) Hydrodynamics: nonscombroid fish. In W.S. Hoar and D.J. Randall, (eds): Fish Physiology. Vol. VII. Locomotion. New York: Academic Press, pp. 189–237.

Webb, P.W. (1978b) Fast-start performance and body form in seven species of teleost fish. J. Exp. Biol. *74:*211–226.

Webb, P.W. (1982) Locomotor patterns in the evolution of actinopterygian fishes. Am. Zool. *22:*329–342.

Webb, P.W. (1984) Body form, locomotion and foraging in aquatic vertebrates. Am. Zool. *24:*107–120.

Weihs, D., and P.W. Webb (1983) Optimization of locomotion. In P.W. Webb and D. Weihs (eds): Fish Biomechanics. New York: Praeger Publishers, pp. 339–371.

Westerfield, M., J.V. McMurray, and J.S. Eisen (1986) Identified moroneurons and their innervation of axial muscles in the zebrafish. J. Neurosci. *6:*2267–2277.

Westneat, M.W., W. Hoese, C. Pell, and S.A. Wainwright (1993) the horizontal spetum: mechanisms of force transfer in locomotion of scombrid fishes (Scombridae, Perciformes). J. Morphol. *217:*183–204.

Williams, T.L., S. Grillner, V.V. Smoljaninov, P. Wallen, S. Kashin, and S. Rossignol (1989) Locomotion in lamprey and trout: the relative timing of activation and movement. J. Exp. Biol. *143:*559–566.